Synthesis of 1,3-Dioxane-Bridged Pyropheophorbide-Diimide and Pyropheophorbide Dimer and Their Intramolecular Electron and Energy Transfer

Atsuhiro Osuka,* Shinji Marumo, Yukihisa Wada, Iwao Yamazaki,† Tomoko Yamazaki,† Yoshihiro Shirakawa,† and Yoshinobu Nishimura†

Department of Chemistry, Faculty of Science, Kyoto University, Kyoto 606

†Department of Chemical Process Engineering, Faculty of Engineering, Hokkaido University, Sapporo 060

(Received January 20, 1995)

1,3-Dioxane-bridged pyropheophorbide–diimide dyads and pyropheophorbide dimer were synthesized by simple acid-catalyzed reactions of methyl pyropheophorbide *d* with diimide-substituted diols and with pentaerythritol, respectively. 1,3-Dioxane-bridged bacteriopyropheophorbide–diimide was similarly prepared from bacteriopyropheophorbide *a*. Intramolecular electron-transfer and energy-transfer reactions in these models have been studied by picosecond fluorescence measurements.

In the bacterial photosynthetic reaction centers (RC), the cyclic tetrapyrrole pigments are held at precise distances and orientations by the protein matrix. With a view to better understanding the mechanism of electron and/or energy transfer in the RC, a large number of artificial models, mainly based on porphyrin molecules, have been extensively studied.[1—3] Recently, increasing attention has been focussed on photosynthetic models with well-defined geometries and energies, since such molecules allow to quantify the distance, orientation, energy-gap dependencies of electron-transfer reactions. In contract to many porphyrin-based models so far developed, there are only a few conformationally restricted models based on natural chlorin-pigments such as chlorophyll or pyropheophorbide.[4] These pigments stand in marked contrast to symmetric porphyrin pigments due to substantially stabilized S_1-energies, strong Qy-absorption band, and unique redox reactivities. Therefore much more systematic studies on these pigments are required for deeper understanding of the electron-transfer reactions in the RC. However, linking electron donor and electron acceptor to a pyropheophorbide or linking two pyropheophorbides in a well defined geometry have been rather difficult, since only limited functional groups are available in the pyropheophorbide structures and introduction of an additional functional group, that is suitable for a link to a redox-active moiety in a conformationally restricted manner, into a pyropheophorbide have been proved rather difficult.[5] Further, the fact that pyropheophorbides are usually much more susceptible to oxidations and degradations in comparison to porphyrins limits the range of the organic transformations in manipulation of pyropheophorbides.

As part of our program employing porphyrin and pyropheophorbide building blocks in the synthesis of photochemically active covalently-linked pigment arrays, we had need of a mild method for linking redox active entities to the pyropheophorbide macrocycles. Here we report simple and convenient synthesis of pyropheophorbide–diimide dyads and pyropheophorbide dimers. The key step is the acid-catalyzed reactions of methyl pyropheophorbide *d* with appropriate diols, by which the 3-formyl group in the methyl pyropheophorbide *d* was converted to a 1,3-dioxane ring through which electron accepting diimide or another pyropheophorbide is attached.[6] This cyclization is mild enough not to affect the ring systems of pyropheophorbide nor bacteriopyropheophorbide. In these models, photoactive entities are bridged by a 1,3-dioxane spacer in a reasonably conformationally restricted manner, which has been indicated by the picosecond time-resolved fluorescence lifetime measurement.

Results and Discussion

Pyropheophorbide–Diimide Dyads. When a mixture of methyl pyropheophorbide *d* (**1**)[4] and 2,2-dimethyl-1,3-propanediol was stirred in the presence of *p*-toluenesulfonic acid (PTS) in CH_2Cl_2, acetal **2** was formed in a quantitative yield (Chart 1). Under these conditions, the 13-carbonyl group of pyropheophorbide does not react with the diol at all. When a solution of **1** in CH_2Cl_2 was stirred in the presence of pyromellitimide (1,2:4,5-benzenetetracarboximide)-substituted 1,3-propanediol **3**, pyropheophorbide–pyromellitimide (H_2P–PIm) dyads were formed as

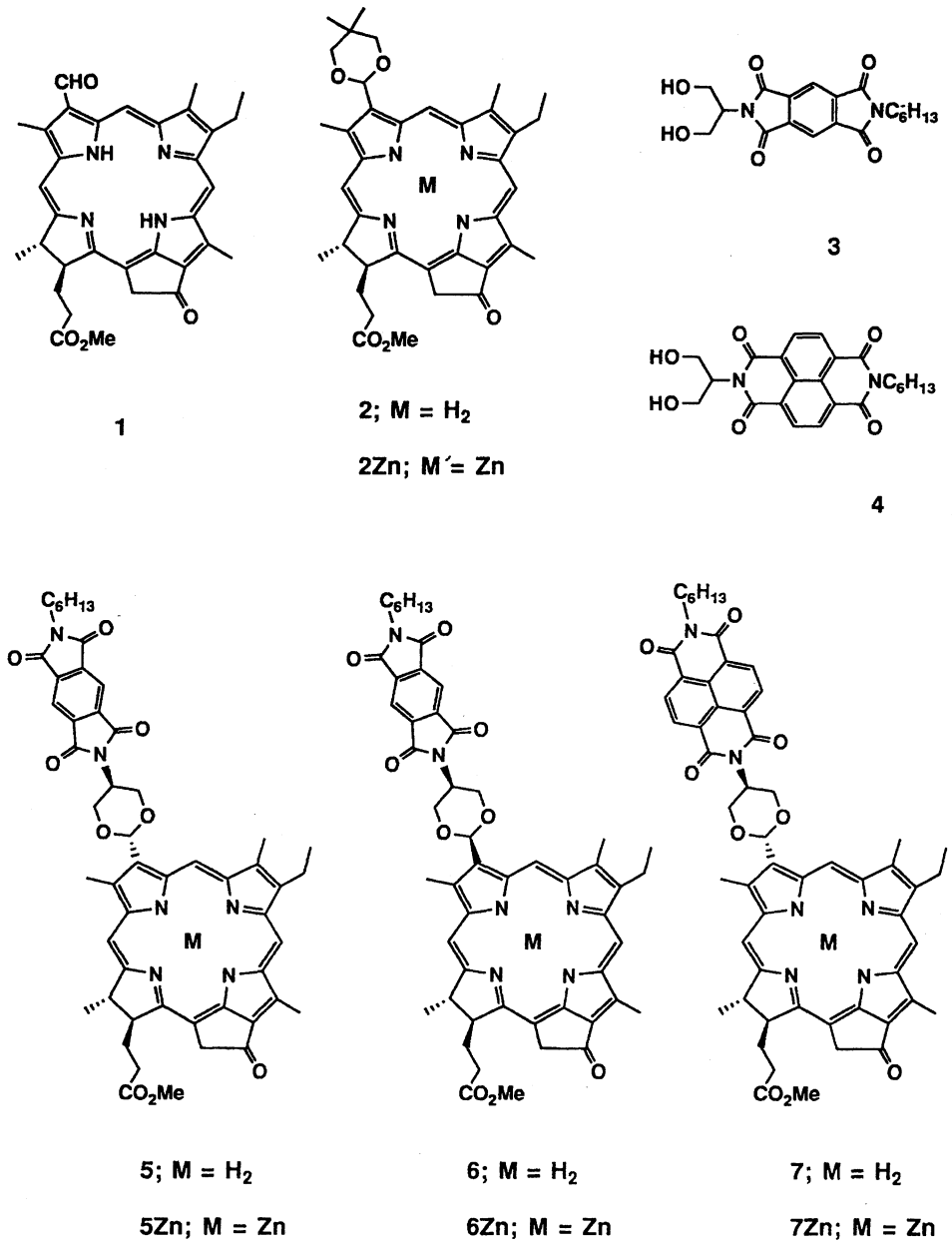

Chart 1.

a mixture of stereoisomers in 79% yield; the ratio of major to minor product was ca. 2. These dyads (**5** and **6**) were separated by flash column chromatography on silica gel. The spectroscopic data including ^{1}H NMR, IR, and mass spectra obtained for these isomers are quite similar to each other. The *N*-methine protons in the 1,3-dioxane ring in the both isomers were coupled with the adjacent vicinal protons with coupling constants of 6.1 and 10.7 Hz in the major product and of 6.2 and 11.5 Hz in the minor one. Observed large coupling constants (>10 Hz) are typical of those for axial–axial or pseudoaxial–pseudoaxial coupling in heterocyclohexane rings,[7] indicating the *N*-methine protons in the both dyads are axial or pseudoaxial. The relative stereochemistry of the products was determined by 1D ROESY difference measurements,[8] through which we assigned the major isomer as trans product **5** and the minor one as cis product **6**. Only in the case of **5**, we observed effective ROESY signals as shown in Fig. 1, irradiation of the acetal methine proton at 7.03 ppm results in the ROESY effect at the protons that are trans to with the *N*-methine proton. Such an effect was not detected for **6**. Presumably, the cis isomer **6** takes a pseudoaxial conformation instead of the chair conformation. The reaction of **1** with 1,8:4,5-naphthalenetetracarboximide (NIm)-substituted 1,3-propanediol **4** in benzene gave NIm–pyropheophorbide dyad **7** only in 11% yield. The yield was improved to 29% by replacing PTS by pyridinium *p*-toluenesulfonate (PPTS). In both cases, only a single product was formed and its stereochemistry was assigned to be trans similarly on the basis of its ROESY difference spectrum.

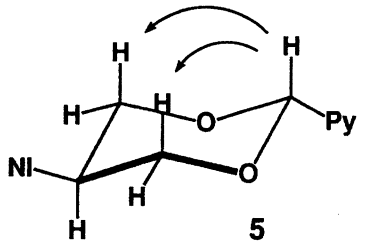

Fig. 1. ROESY effects observed for **5**. NI and Py indicate pyromellitimide and pyropheophorbide moieties, respectively.

The fluorescence lifetime and relative fluorescence quantum yield of these diimide–pyropheophorbides are listed in Table 1. The fluorescence of the pyropheophorbide moiety (H_2P) in **5** and **6** is not quenched in benzene, THF, or DMF, while the fluorescence of the pyropheophorbide moiety in the dyads **5Zn**, **6Zn**, **7**, and **7Zn**, is quenched by the attached diimide, suggesting the occurrence of intramolecular charge separation. With exception of the fluorescence of **5Zn** and **6Zn** in benzene that exhibits a biphasic decay, the other fluorescence decay curves of $^1(P)^*$ can be analyzed by a single exponential function. In the case of single exponential decay, rates of charge separation (k_{CS}) are calculated by the equation; $k_{CS}=1/\tau-1/\tau_0$, where τ and τ_0 are the fluorescence lifetime of pyropheophorbide–diimide and that of diimide-free reference pyropheophorbide, respectively (Scheme 1a). On the other hand, the biphasic decay observed for **5Zn** and **6Zn** in benzene indicates the reaction scheme shown in Scheme 1b, where a rapid equilibrium between the excited state $^1(P)^*$–Im and an ion pair state $(P)^+$–$(Im)^-$ is achieved.[9—11] This equilibrium may be possible when the energy levels of the excited state and ion pair state are close to each other. Assuming this thermal repopulation of the $^1(P)^*$–Im from $(P)^+$–$(Im)^-$, k_{CS} have been calculated according to the well-established procedure.[9—11] Through this analysis, rates of back electron transfer (k_{-CR}) and charge recombination (k_{CS}) are simultaneously calculated; $k_{-CS}=1.5\times10^8$ s^{-1} and $k_{CR}=5.3\times10^8$ s^{-1} for **5Zn** and $k_{-CS}=2.2\times10^8$ s^{-1} and $k_{CR}=5.8\times10^8$ s^{-1} for **6Zn**. Nearly identical ET rates have been obtained for the two isomers.[12] It is notable that k_{CS} values are almost independent of the solvent polarity, being the same as those observed for distance-fixed dyads.[11,13] This result can be qualitatively accounted for in a similar manner as follows. In general, the decrease of the solvent polarity is followed by decreases in both of a free energy gap for the CS reaction and solvent reorganization energy. Therefore these two effects compensate each other, resulting in rather con-

Table 1. Fluorescence Lifetime and Rate of Charge Separation in P–Im Dyads

Compound	Solvent	Φ[a]	Lifetime[b]	k_{CS}[c]	$-\Delta G°$[d]
			ns	s^{-1}	eV
5Zn	Benzene	0.63	1.13(47) 2.35(53)	3.7×10^8	ca. 0
	THF	0.40	1.50	4.4×10^8	0.26
	DMF	0.42	1.62	4.0×10^8	0.47
6Zn	Benzene	0.65	0.99(52) 2.36(49)	3.7×10^8	ca. 0
	THF	0.40	1.49	4.4×10^8	0.26
	DMF	0.40	1.65	3.9×10^8	0.47
7	Benzene	0.081	0.45	2.1×10^9	0.05
	THF	0.19	1.64	4.9×10^8	0.28
	DMF	0.30	2.29	3.1×10^8	0.49
7Zn	Benzene	0.026	0.43	2.1×10^9	0.30
	THF	0.024	0.10	9.8×10^9	0.56
	DMF	0.045	0.14	6.9×10^9	0.77

a) Fluorescence quantum yield relative to the Im-free reference compound, ±5%. b) Fluorescence lifetime determined by single photon counting technique, ±5%. Numbers in parentheses are relative amplitudes of pre-exponential functions. c) Rates of the intramolecular charge separation calculated on the basis of the fluorescence lifetime. The fluorescence lifetimes of the Im-free reference compounds are 3.7 (benzene), 4.4 (THF), and 4.7 (DMF) ns for **2Zn**, and 7.8 (benzene), 8.3 (THF), and 7.9 (DMF) ns for **2**, respectively. Details are given in the text. d) Energy gap for the CS. Energies in THF and DMF are determined by Born equation: A. Weller, *Z. Phys. Chem.* (*N.Y.*), **133**, 93 (1982).

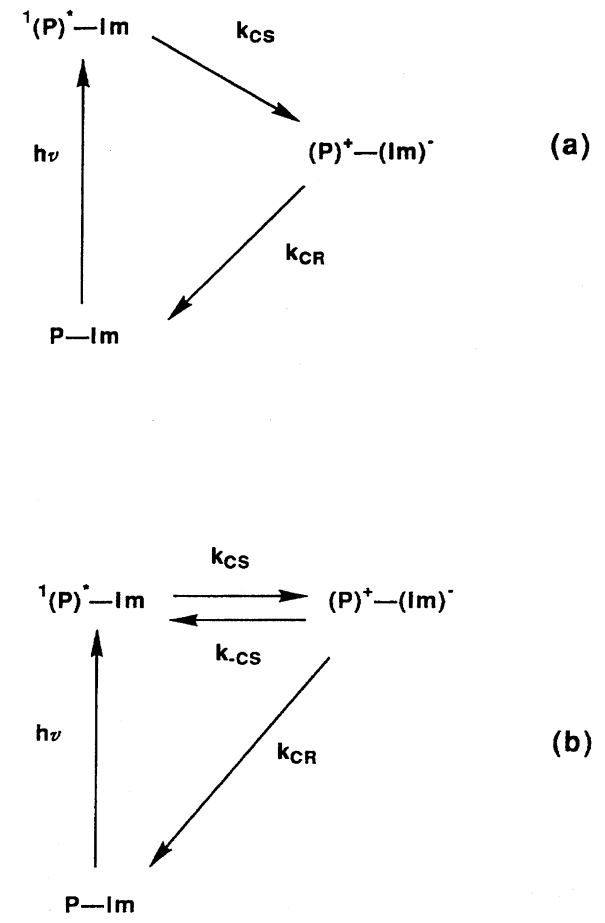

Scheme 1.

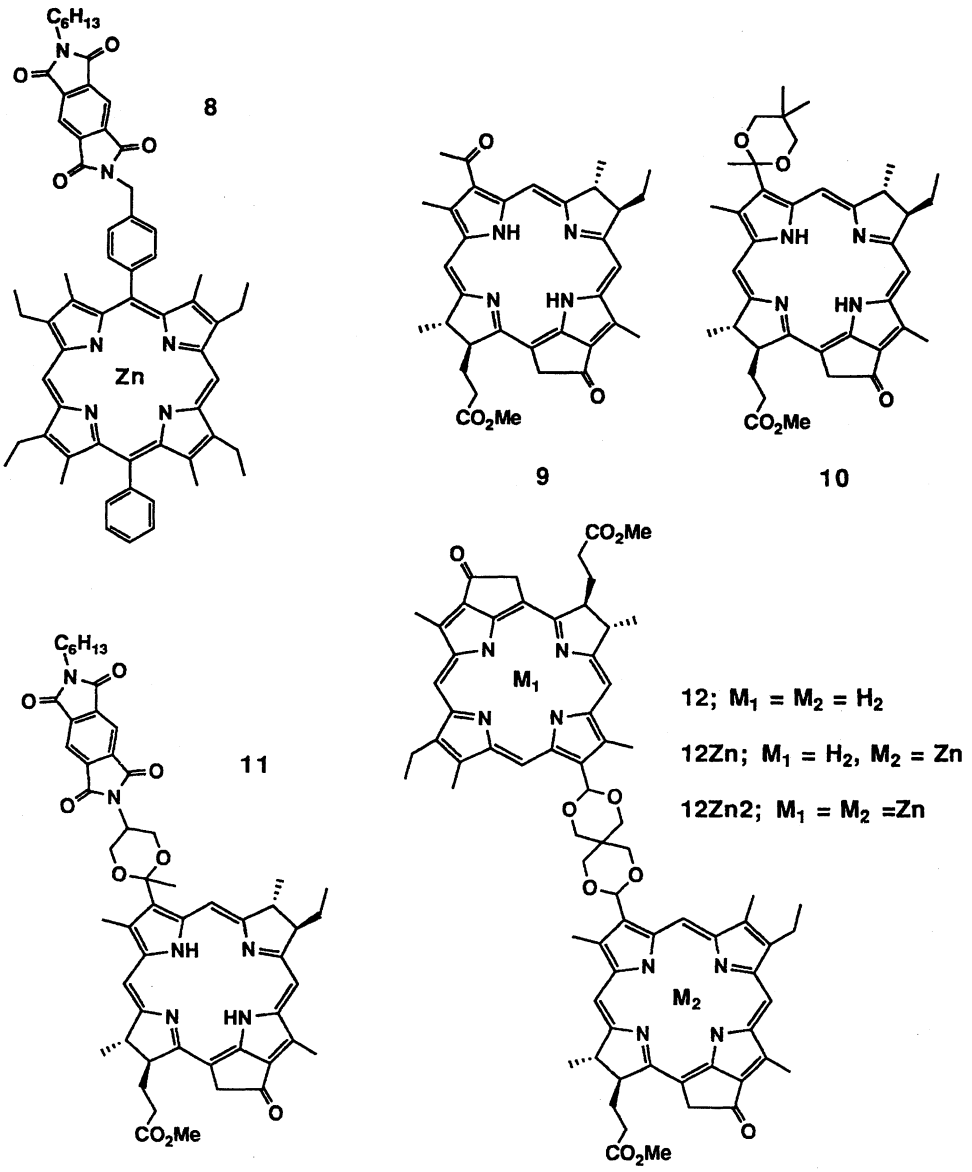

Chart 2.

stant k_{CS} values independent of solvent polarity. The biphasic decay behaviors of **5Zn** and **6Zn** in benzene provide the rates of the charge recombination (CR) reaction of the ion-pair to the ground state. The energy gap for these CR reaction can be estimated to be ca. 1.89 eV, since the energy level of the ion-pair should be nearly the same as that of the S_1-state (1.89 eV). In spite of these large energy gaps, it is of mechanistic interest that the ion-pair formed from these models undergoes relatively efficient CR reaction to the ground state. Usually the CR reactions of covalently-linked ion-pairs are lying in the Marcus inverted region, where a larger energy gap leads to a smaller k_{CR} rate. When the ratio of k_{CS}/k_{CR} is taken as an index of charge-separation efficiency of photosynthetic models, ratios of 0.6—0.7 are calculated for **5Zn** and **6Zn**, while more than 40 for the related pyromellitimide-linked zinc-porphyrin **8** which has almost the same the energy gap but bears a 1,4-phenylene-methylene spacer.[13] This analysis may reveal that a 1,4-phenylene-methylene spacer is superior to a 1,3-dioxane spacer in attaining a high k_{CS}/k_{CR} ratio. Systematic studies on these spacer dependencies of k_{CS}/k_{CR} ratio will provide a useful basis for the future design of photosynthetic models.

Bacteriopyropheophorbide– Diimide Dyad. This acetal method has been also applied to a bacteriopyropheophorbide system. When a mixture of methyl bacteriopyropheophorbide *a* (**9**)[14] and 2,2-dimethyl-1,3-propanediol was stirred in the presence of PTS in CH_2Cl_2, acetal **10** was formed in 44% yield (Chart 2). In the same manner, bacteriopyropheophorbide–pyromellitimide **11** was obtained from the reaction of **9** with **3** in 21% yield. In this case again, only a single isomer was isolated. The stereochemistry of the 1,3-dioxane ring was determined to be trans on the basis of its ROESY difference spectrum that is quite similar

to that of **5**. The fluorescence intensity of **11** relative to that of **10** is ca. 0.2 in benzene, THF, and DMF, indicating the intramolecular electron transfer to the attached pyromellitimide with similar rates.

Pyropheophorbide Dimer. Finally the acetal-formation reaction provides a new pyropheophorbide dimer in a single step. Thus, the reaction of **1** with 0.5 equivalent amount of pentaerythritol gave dimer **12** cleanly as a single product in 71% yield. In **12**, two pyropheophorbide chromophores are held at an extended conformation with the center-to-center distance of ca. 25 Å. Biszinc- and monozinc complexes **12Zn** and **12Zn2** were prepared from **12** by the reaction with $Zn(OAc)_2$ followed by chromatographic separation. The chemical shifts of **12**, **12Zn**, and **12Zn2** are almost identical with those in **2** and **12Zn**, indicating an extended conformation again. The absorption and fluorescence spectra of **12** and **12Zn2** are identical with those of **2** and **2Zn**. In the hybrid dimer **12Zn**, reversible singlet excitation energy transfer between the ZnP and H_2P has been revealed by the fluorescence lifetime measurements. The fluorescence decays of **12** and **12Zn2** in THF can be fit with single exponential functions with time constants of 8.5 and 4.5 ns, respectively, being practically the same as those of **2** and **2Zn**. The steady-state fluorescence spectrum of **12Zn** in THF contains the emission from both the H_2P (at 650 nm) and ZnP moieties (at 665 nm), which decays with a time constant of ca. 6.1 ns at the both wavelength. These results indicate a rapid equilibrium between $^1(H_2P)^*$–ZnP and H_2P–$^1(ZnP)^*$. In other words, the singlet energy-transfer reactions of $^1(H_2P)^*$–ZnP$\rightleftarrows$$H_2P$–$^1(ZnP)^*$ are much faster than the respective intrinsic decay of the singlet excited state. This is consistent with a small energy difference (ca. 0.03 eV) between the two singlet excited states and the large spectral overlap in the energy transfer in the both directions.

In summary, the acetal formation can be used for attachment of photoactive functional groups to pyropheophorbide and bacteriopyropheophorbide under mild conditions. A 1,3-dioxane bridge holds the photoactive entities with certain conformational rigidities. Further applications of this stategy to connecting other photoactive moieties such as quinones, porphyrins, and carotenoids are being conducted in our laboratory.

Experimental

General Methods. The instruments and procedures were as previously reported.[12] Methyl pyropheophorbide *d* (**1**) was prepared from methyl pyropheophorbide *a* according to the method reported by Wasielewski.[14] Methyl pyropheophorbide *a* was purified in large scale from Spirulina (Nippon Ink).

Acetal 2. A mixture of **1** (55 mg, 0.1 mol), neopentyl alcohol (31 mg, 0.3 mmol), and PTA (38 mg) in CH_2Cl_2 (20 ml) was stirred for 2 h. The reaction mixture was poured into H_2O (100 ml). The organic layer was separated and washed with aqueous $NaHCO_3$ solution. Removal of the solvent by the rotary evaporator gave almost pure acetal **2**, which was purified by short silica gel column in 95% yield.

2. ^{1}H NMR ($CDCl_3$) δ=−1.83 (s, 1H, NH), 0.15 (s, 1H, NH), 1.07 (s, 3H, Acetal-CH_3), 1.65 (t, 3H, 8^2-CH_3), 1.82 (d, 3H, 18-CH_3), 1.86 (s, 3H, Acetal-CH_3), 2.28—2.36, 2.56—2.67 (m, 2H+2H, 17-CH_2CH_2), 3.28, 3.49, 3.60, 3.69 (each s, 3H, 2-, 7-, 12-CH_3, CO_2CH_3), 3.71 (dq, 2H, J=8 Hz, 8-CH_2), 4.08, 4.15 (dd, 4H, J=11 Hz, Acetal-OCH_2), 4.29 (dt, 1H, 17-H), 4.48 (dq, 1H, 18-H), 5.15, 5.31 (d, 1H+1H, J=20 Hz, 13^2-H), 6.80 (s, 1H, 3-CH), 8.57 (s, 1H, *meso*-H), 9.54 (s, 1H, *meso*-H), 9.93 (s, 1H, *meso*-H). IR (KBr) ν_{max} 1735 (CO_2CH_3), 1682 cm^{-1} (C=O). MS (FAB) Found: m/z 637. Calcd for $C_{38}H_{44}N_4O_5$: M^+, 637.

2Zn. ^{1}H NMR ($CDCl_3$) δ=1.26 (s, 3H, Acetal-CH_3), 1.56 (s, 3H, Acetal-CH_3), 1.65 (t, 3H, 8^2-CH_3), 1.85 (d, 3H, 18-CH_3), 2.20—2.30, 2.43—2.57 (m, 2H+2H, 17-CH_2CH_2), 3.10, 3.14, 3.42, 3.43 (each s, 3H, 2-, 7-, 12-CH_3, CO_2CH_3), 3.50 (m, 2H, 8-CH_2), 3.61 (m, 4H, Acetal-OCH_2), 4.17 (dt, 1H, 17-H), 4.40 (dq, 1H, 18-H), 4.68, 4.83 (d, 1H+1H, J=20 Hz, 13^2-H), 6.30 (s, 1H, 3-CH), 8.52 (s, 1H, *meso*-H), 9.29 (s, 1H, *meso*-H), 9.55 (s, 1H, *meso*-H). IR (KBr) ν_{max} 1720, 1685 cm^{-1} (C=O). MS (FAB) Found: m/z 698. Calcd for $C_{38}H_{42}N_4O_5Zn$, M^+, 698.

Diols **3** and **4** were prepared by heating a 1 : 1 : 1 mixture of serinol, pyromellitimide anhydride or 1,8 : 4,5-naphthalenetetracarboxylic anhydride, and hexylamine in DMF at 120 °C. Yields of **3** and **4** are 35 and 22%, respectively.

3. Mp 198—200 °C. ^{1}H NMR ($CDCl_3$) δ=0.87 (t, 3H, *n*-Hex-6-CH_3), 1.28 (m, 2H, *n*-Hex-5-CH_2) 1.32 (m, 2H, *n*-Hex-4-CH_2), 1.48 (m, 2H, *n*-Hex-3-CH_2), 1.69 (m, 2H, *n*-Hex-2-CH_2), 2.74 (s, 2H, OH), 3.72 (t, 2H, *n*-Hex-1-CH_2), 4.07 (dd, 2H, OCH_2), 4.12 (m, 2H, OCH_2), 4.48 (m, 1H, NCH), 8.26 (s, 2H, PIm-Ar-H). IR (KBr) ν_{max} 3382 (OH), 1712 cm^{-1} (C=O). MS (FAB) Found: m/z 375. Calcd for $C_{19}H_{22}O_6N_2$: M^++1, 375. Found: C, 60.71; H, 5.93; N, 7.51%. Calcd for $C_{19}H_{22}N_2O_6$: C, 60.95; H, 5.92; N, 7.48%.

4. Mp 240—242 °C. ^{1}H NMR ($CDCl_3$) δ=0.87 (t, 3H, J=7 Hz, *n*-Hex-CH_3), 1.33 (m, 2H, *n*-Hex-5-CH_2), 1.36 (m, 2H, *n*-Hex-4-CH_2), 1.43 (m, 2H, *n*-Hex-3-CH_2), 1.74 (m, 2H, *n*-Hex-2-CH_2), 2.85 (s, 2H, OH), 4.15 (m, 4H+2H, $2CH_2OH$, *n*-Hex-1-CH_2), 5.49 (m, 1H, NCH), 8.75 (s, 4H, NIm-Ar-H). IR (KBr) ν_{max} 3382 (OH), 1658 cm^{-1} (C=O). MS (FAB) Found: m/z 425. Calcd for $C_{23}H_{24}O_6N_2$: M^++1, 425. Found: C, 65.25; H, 5.86; N 6.59%. Calcd for $C_{23}H_{24}N_2O_6$: C, 65.08; H, 5.86; N, 6.59%.

Pyromellitimide–Pyropheophorbide Dyads. A mixture of **1** (55 mg, 0.1 mol), the diol **3** (75 mg, 0.2 mmol), and PTA (38 mg) in CH_2Cl_2 (20 ml) was stirred at room temperature overnight. The reaction mixture was poured into H_2O (100 ml). The organic layer was separated and washed with aqueous $NaHCO_3$ solution. After removal of the solvent by the rotary evaporator, the product **5** (72 mg, 79%) was separated by flash silica gel column (eluting with a mixture of methanol and CH_2Cl_2 (0.05/99.5)). Zinc complex **5Zn** was prepared by the reaction of **5** with $Zn(OAc)_2$.

5. ^{1}H NMR ($CDCl_3$) δ=−2.09 (s, 1H, NH), −0.13 (s, 1H, NH), 0.87 (t, 3H, *n*-Hex-CH_3), 1.28 (m, 6H, *n*-Hex-5-CH_2), 1.30 (m, 2H, *n*-Hex-4-CH_2), 1.33 (m, 2H, *n*-Hex-3-CH_2), 1.78 (t, 3H, 8^2-CH_3), 1.88 (d, 3H, 18-CH_3), 2.30—2.43, 2.59—2.82 (m, 2H+2H, 17-CH_2CH_2), 3.36, 3.59, 3.64, 3.67 (each s, 3H, 2-, 7-, 12-CH_3, CO_2CH_3), 3.60 (t, 2H, *n*-Hex-1-CH_2), 3.74 (m, 2H, 8-CH_2), 4.35 (dt, 1H, 17-H),

4.55 (dq, 1H, 18-H), 4.64 (dd, 2H, J=6.1, 10.7 Hz, Acetal-OCH_2), 4.94 (m, 2H, Acetal-OCH_2), 5.09 (m, 1H, NCH), 5.07, 5.24 (d, 1H+1H, 13^2-H), 7.03 (s, 1H, 3-CH), 7.37 (s, 2H, PIm-Ar-H), 8.68 (s, 1H, *meso*-H), 9.47 (s, 1H, *meso*-H), 9.77 (s, 1H, *meso*-H). IR (KBr) ν_{max} 1720, 1695 cm^{-1} (C=O). MS (FAB) Found: m/z 907. Calcd for $C_{52}H_{54}N_6O_9$: M^++1, 907.

5Zn. ^{1}H NMR ($CDCl_3$) δ=0.89 (t, 3H, *n*-Hex-CH_3), 1.25—1.35 (m, 6H, *n*-Hex-5-, 4-, 3-CH_2), 1.64 (m, 2H, *n*-Hex-2-CH_2), 1.72 (t, 3H, 8^2-CH_3), 1.85 (d, 3H, 18-CH_3), 2.35—2.40, 2.50—2.66 (m, 2H+2H, 17-CH_2CH_2), 3.32, 3.44, 3.48, 3.60 (each s, 3H, 2-, 7-, 12-CH_3, CO_2CH_3), 3.62 (t, 2H, *n*-Hex-1-CH_2), 3.73 (m, 2H, 8-CH_2), 4.27 (dt, 1H, 17-H), 4.51 (dq, 1H, 18-H), 4.52 (m, 2H, Acetal-OCH_2), 4.96 (m, 2H, Acetal-OCH_2), 5.07, 5.23 (d, J=20 Hz, 1H+1H, 13^2-H), 5.19 (m, 1H, NCH), 6.89 (s, 1H, 3-CH), 8.04 (s, 2H, PIm-Ar-H), 8.52 (s, 1H, *meso*-H), 9.49 (s, 1H, *meso*-H), 9.59 (s, 1H, *meso*-H). IR (KBr) ν_{max} 1718, 1685 cm^{-1} (C=O). MS (FAB) Found: m/z 969. Calcd for $C_{52}H_{52}N_6O_9Zn$: M^+, 969.

6. ^{1}H NMR ($CDCl_3$) δ=−2.01 (s, 1H, NH), −0.06 (s, 1H, NH), 0.88 (t, 3H, *n*-Hex-CH_3), 1.27—1.35 (m, 6H, *n*-Hex-5-, 4-, 3-CH_2), 1.58 (m, 2H, *n*-Hex-2-CH_2), 1.77 (t, 3H, 8^2-CH_3), 1.86 (d, 3H, 18-CH_3), 2.28—2.40, 2.56—2.81 (m, 2H+2H, 17-CH_2CH_2), 3.36, 3.58, 3.63, 3.69, (each s, 3H, 2-, 7-, 12-CH_3, CO_2CH_3), 3.67 (t, 2H, *n*-Hex-1-CH_2), 3.75 (m, 2H, 8-CH_2), 4.43 (dt, 1H, 17-H), 4.54 (dq, 1H, 18-H), 4.63 (dd, 2H, J=6.2, 11.5 Hz, Acetal-OCH_2), 5.00 (m, 2H, Acetal-OCH_2), 5.13 (m, 1H, NCH), 5.18, 5.35 (d, 1H+1H, J=20 Hz, 13^2-H), 7.06 (s, 1H, 3-CH), 7.75 (s, 2H, PIm-Ar-H), 8.66 (s, 1H, *meso*-H), 9.52 (s, 1H, *meso*-H), 9.79 (s, 1H, *meso*-H), IR (KBr) ν_{max} 1718, 1685 cm^{-1} (C=O). MS (FAB) Found: m/z 907. Calcd for $C_{52}H_{54}N_6O_9$: M^++1, 907.

6Zn. ^{1}MH NMR ($CDCl_3$) δ=0.90 (t, 3H, *n*-Hex-CH_3), 1.25—1.32 (m, 6H, *n*-Hex-5-, 4-, 3-CH_2), 1.68 (m, 2H, *n*-Hex-2-CH_2), 1.73 (t, 3H, 8^2-CH_3), 1.84 (d, 3H, 18-CH_3), 2.24—2.42, 2.50—2.67 (m, 2H+2H, 17-CH_2CH_2), 3.35, 3.46, 3.49, 3.64 (each s, 3H, 2-, 7-, 12-CH_3, CO_2CH_3), 3.70 (t, 2H, *n*-Hex-1-CH_2), 3.77 (dq, 2H, 8-CH_2), 4.29 (dt, 1H, 17-H), 4.53 (dq, 1H, 18-H), 4.53 (m, 2H, Acetal-OCH_2), 5.01 (m, 2H, Acetal-OCH_2), 5.02, 5.19 (d, 1H+1H, 13^2-H), 5.23 (m, 1H, NCH), 6.94 (s, 1H, 3-CH), 8.19 (s, 2H, PIm-Ar-H), 8.51 (s, 1H, *meso*-H), 9.56 (s, 1H, *meso*-H), 9.66 (s, 1H, *meso*-H). IR (KBr) ν_{max} 1720, 1690 cm^{-1} (C=O). MS (FAB) Found: m/z 969. Calcd for $C_{52}H_{52}N_6O_9$: M^+, 969.

1,8 : 4,5-Naphthalenetetracarboxamide–Pyropheophorbide Dyad. A mixture of **1** (32 mg, 0.06 mol), **4** (54 mg, 0.13 mmol), and PPTS (32 mg) in dry benzene (35 ml) was refluxed with Dean–Stark apparatus for 10 h under nitrogen atmosphere. The reaction mixture was poured into H_2O (100 ml). The organic layer was separated and was washed with aqueous $NaHCO_3$ solution. After removal of the solvent by the rotary evaporator, the product **7** was separated by flash silica gel column (eluting with a mixture of methanol and CH_2Cl_2 (0.05/99.5)) in 29% yield.

7. ^{1}H NMR ($CDCl_3$) δ=−2.55 (s, 1H, NH), −0.55 (s, 1H, NH), 0.87 (t, 3H, *n*-Hex-6-CH_3), 1.26 (m, 2H, *n*-Hex-5-CH_2), 1.30 (m, 2H, *n*-Hex-4-CH_2), 1.60 (m, 2H, *n*-Hex-3-CH_2), 1.78 (m, 2H, *n*-Hex-2-CH_2), 1.96 (t, 3H, 8^2-CH_3), 1.98 (d, 3H, 18-CH_3), 2.40—2.57, 2.65—2.87 (m, 2H+2H, 17-CH_2CH_2), 3.67, 3.69, 3.70, 3.75 (each s, 3H, 2-, 7-, 12-CH_3, CO_2CH_3), 3.72 (m, 2H, 8-CH_2), 3.78 (t, 3H, *n*-Hex-1-CH_2), 4.40 (dt, 1H, 17-H), 4.60 (dq, 1H, 18-H), 4.82 (m, 2H, Acetal-OCH_2), 5.19, 5.36 (d, 1H+1H, 13^2-H), 5.43 (m, 2H, Acetal-OCH_2), 6.08 (m, 1H, NCH), 7.18 (s, 1H, 3-CH), 7.51 (d, 2H, J=8 Hz, NIm-Ar-H), 7.63 (d, 2H, J=8 Hz, NIm-Ar-H), 8.71 (s, 1H, *meso*-H), 9.23 (s, 1H, *meso*-H), 9.72 (s, 1H, *meso*-H). IR (KBr) ν_{max} 1705, 1668 cm^{-1} (C=O). MS (FAB) Found: m/z 957. Calcd for $C_{56}H_{56}N_6O_9$: M^++1, 956.

7Zn. ^{1}H NMR ($CDCl_3$) δ=0.85 (t, 3H, *n*-Hex-CH_3), 1.15—1.25 (m, 6H, *n*-Hex-5-, 4-, 3-CH_2), 1.67 (t, 3H, 8^2-CH_3), 1.78 (m, 2H, *n*-Hex-2-CH_2), 1.92 (d, 2H, 18-CH_3), 2.17—2.33, 2.40—2.58 (m, 2H, 17-CH_2CH_2), 3.48, 3.34, 3.56, 3.67 (each s, 3H, 2-, 7-, 12-CH_3, CO_2CH_3), 3.51 (t, 2H, *n*-Hex-1-CH_2), 3.70 (m, 2H, 8-CH_2), 4.35 (dt, 1H, 17-H), 4.54 (m, 1H, 18-H), 4.79 (m, 2H, Acetal-OCH_2), 5.06, 5.23 (d, 1H+1H, J=20 Hz, 13^2-H), 5.48 (m, 2H, Acetal-OCH_2), 6.23 (m, 1H, NCH), 7.73 (d, 2H, J=8 Hz, NIm-Ar-H), 8.36 (d, 2H, J=8 Hz, NIm-Ar-H), 8.57 (s, 1H, *meso*-H), 9.37 (s, 1H, *meso*-H), 9.64 (s, 1H, *meso*-H). IR (KBr) ν_{max} 1705, 1665 cm^{-1} (C=O). MS (FAB) Found: m/z 1019. Calcd for $C_{56}H_{54}N_6O_9Zn$: M^+, 1019.

Bacteriopyropheophorbide *a* methyl ester (**9**) was prepared by methylation of bacteriopyropheophorbide *a* under Mukaiyama conditions.[15] Bacteriopyropheophorbide *a* was prepared according to the literature[14] with several modifications. Bacteriochlorophyll *a* obtained from the culture of *Rhodopseudomonas sphaeroides* was first dematalled (0.1 M HCl, 10 min, room temperature, 1 M=1 mol dm^{-3}) and then decarboxylated (collidine, reflux, 3 h), and finally hydrolyzed (TFA, 2 h, room temperature) to give bacteriopyropheophorbide *a*.

9. ^{1}H NMR ($CDCl_3$) δ=−1.03 (s, 1H, NH), 0.35 (s, 1H, NH), 1.11 (t, 3H, J=8 Hz, 8^2-CH_3), 1.72, 1.78 (each d, 3H, J=7 Hz, 7-CH_3, 18-CH_3), 2.04—2.39, 2.48—2.62 (m, 6H, 8-CH_2, 17-CH_2CH_2), 3.17 (s, 3H, 3-CH_3), 3.45 (s, 3H, 12-CH_3), 3.50 (s, 3H, 2-CH_3), 3.62 (s, 3H, CO_2CH_3), 4.03, 4.12, 4.30 (each m, 1H+1H+2H, 7-, 8-, 17-, 18-H), 4.91, 5.12 (d, 1H+1H, J=20 Hz, 13^2-H), 8.42 (s, 1H, 20-H), 8.47 (s, 1H, 10-H), 8.99 (s, 1H, 5-H). MS (FAB) Found: m/z 568. Calcd for $C_{34}H_{38}N_4O_4$: M^++1, 568.

Bacteriopyropheophorbide Acetal 10. A mixture of **9** (9 mg, 16 μmol), neopentyl alcohol (5 mg), and PTA (7.2 mg) in CH_2Cl_2 (5 ml) was refluxed for 3 h. The reaction mixture was poured into H_2O (100 ml). The organic layer was separated and washed with aqueous $NaHCO_3$ solution. After removal of the solvent by the rotary evaporator, separation by silica gel column gave acetal **10** in 44% yield.

10. ^{1}H NMR ($CDCl_3$) δ=−0.29 (s, 1H, NH), 0.54 (s, 3H, Acetal-CH_3), 1.12 (t, 3H, 8^2-CH_3), 1.48 (s, 3H, Acetal-CH_3), 1.68, 1.72 (each d, 3H, 7-, 18-CH_3), 2.09 (s, 3H, 3-CH_3), 1.97—2.14, 2.17—2.32, 2.41—2.64 (m, 6H, 8-CH_2, 17-CH_2CH_2), 3.25, 3.35, 3.61 (each s, 3H, 2-, 12-, CO_2CH_3), 3.84 (m, 2H, Ketal-OCH_2), 3.90, 4.03, 4.10, 4.14 (each m, 1H, 7-, 8-, 17-, 18-H), 4.78, 5.00 (d, 1H+1H, J=20 Hz, 13^2-H), 8.10 (s, 1H, *meso*-H), 8.23 (s, 1H, *meso*-H), 8.95 (s, 1H, *meso*-H). MS (FAB) Found: m/z 652. Calcd for $C_{39}H_{48}N_4O_5$: M^++1, 652.

Pyromellitimide–Bacteriopyropheophorbide Dyad. A mixture of **9** (9 mg, 16 μmol), **3** (12 mg, 32 μmol), and PTA (7.2 mg) in CH_2Cl_2 (20 ml) was refluxed for 3 h. The reaction mixture was poured into H_2O (100 ml). The organic layer was separated and washed with aqueous

$NaHCO_3$ solution. After removal of the solvent by the rotary evaporator, the product **11** (3 mg, 21%) was separated by flash silica gel column (eluting with a mixture of methanol and CH_2Cl_2 (0.05/99.5)).

11. ^{1}H NMR ($CDCl_3$) δ=−0.34 (s, 1H, NH), 0.81 (t, 3H, *n*-Hex-CH_3), 1.10 (m, 3H+2H, 8^2-CH_3, *n*-Hex-5-CH_2), 1.23 (m, 4H, *n*-Hex-5-, 4-CH_2), 1.63 (m, 4H, *n*-Hex-3-, 2-CH_2), 1.72 (each d, 3H, 7-CH_3, 18-CH_3), 1.98—2.07, 2.12—2.35, 2.48—2.60 (m, 6H, 8-CH_2, 17-CH_2CH_2), 2.11 (s, 3H, 3-CH_3), 3.30, 3.35, 3.62 (s, 3H, 2-, 12-, CO_2CH_3), 3.63 (t, 3H, *n*-Hex-1-CH_2), 3.87, 4.02, 4.10, 4.13 (each m, H, 7-, 8-, 17-, 18-H), 4.20 (m, 2H, Ketal-OCH_2), 4.76 (m, 2H, Ketal-OCH_2), 4.80, 5.01 (d, 1H+1H, J=20 Hz, 13^2-H), 8.00 (s, 2H, PIm-Ar-H), 8.17 (s, 1H, *meso*-H), 8.25 (s, 1H, *meso*-H), 8.89 (s, 1H, *meso*-H). IR (KBr) ν_{max} 1724 (CO_2CH_3), 1695 cm^{-1} (C=O). MS (FAB) Found: m/z 923. Calcd for $C_{53}H_{58}N_6O_9$: M^++1, 923.

Pyropheophorbide Dimer. A mixture of **1** (22 mg, 0.04 mol), pentaerythritol (2 mg, 0.02 mmol), and PTA (7.6 mg) in CH_2Cl_2 (20 ml) was stirred at room temperature overnight. The reaction mixture was poured into H_2O (100 ml). The organic layer was separated and was washed aqueous $NaHCO_3$ solution. After removal of the solvent by the rotary evaporator, the product **12** was separated by flash silica gel column (eluting with a mixture of methanol and CH_2Cl_2 (0.05/99.5)) in 71% yield.

12. ^{1}H NMR ($CDCl_3$) δ=−1.83 (s, 2H, NH), 0.30 (s, 2H, NH), 1.83 (t, 6H, 8^2-CH_3), 1.85 (d, 6H, 18-CH_3), 2.17—2.35, 2.55—2.71 (m, 8H, 17-CH_2CH_2), 3.26, 3.61, 3.63, 3.69 (each s, 6H, 2-, 7-, 12-CH_3, CO_2CH_3), 3.66 (m, 4H, 8-CH_2), 4.35 (d, 4H, J=12 Hz, Acetal-OCH_2), 4.55 (m, 4H, 17-H, 18-H), 4.74 (d, 2H, J=12 Hz, Acetal-OCH_2), 5.12 and 5.33 (d, 4H, J=20 Hz, 13^2-H), 5.99 (d, 2H, Acetal-OCH_2), 7.08 (s, 2H, 3-CH), 8.67 (s, 2H, *meso*-H), 9.55 (s, 2H, *meso*-H), 9.90 (s, 2H, *meso*-H), IR (KBr) ν_{max} 1735 (CO_2CH_3), 1697 cm^{-1}. MS (FAB) Found: m/z 1202. Calcd for $C_{71}H_{76}N_8O_{10}$: M^++2, 1202.

12Zn. ^{1}H NMR ($CDCl_3$) δ=−1.85 (s, 1H, NH), 0.27 (s, 1H, NH), 1.65 (m, 6H, 8^2, 8^{2Zn}-CH_3), 1.83 (m, 6H, 18-CH_3, 18^{Zn}-CH_3), 2.16—2.37, 2.41—2.71 (m, 8H, 17-CH_2CH_2, 17^{Zn}-CH_2CH_2), 3.32, 3.35, 3.45, 3.59, 3.62, 3.63, 3.68, 3.71 (each s, 3H, 2-, 7-, 12-CH_3, 17-CO_2CH_3, 2^{Zn}-, 7^{Zn}-, 12^{Zn}-CH_3, 17^{Zn}-CO_2CH_3), 3.52 (d, 2H, Acetal-OCH_2), 3.74 (m, 4H, 8-CH_2), 4.30 (m, 4H, 17-H, 18-H, 17^{Zn}-H, 18^{Zn}-H), 4.46 (m, 2H, Acetal-OCH_2), 4.70 (t, 2H, Acetal-OCH_2), 5.00—5.31 (d, 4H, 13^2-H+13^{Zn-2}-H), 6.00 (m, 2H, Acetal-OCH_2), 6.98, 7.08 (each d, 1H, 3-CH, 3^{Zn}-CH), 8.53, 8.64, 9.53, 9.55, 9.84, 9.87 (each s, 1H, *meso*-H, *meso*^{Zn}-H). IR (KBr) ν_{max} 1735 (CO_2CH_3), 1689 cm^{-1} (C=O). MS (FAB) Found: m/z 1264. Calcd for $C_{71}H_{74}H_8O_{10}Zn$: M^++1, 1264.

12Zn2. ^{1}H NMR ($CDCl_3$) δ=1.57 (t, 6H, 8^2-CH_3), 1.85 (d, 6H, 18-CH_3), 2.20—2.33, 2.43—2.58 (m, 8H, 17-CH_2CH_2), 3.39, 3.44, 3.50, 3.52 (each s, 6H, 2-, 7-, 12-CH_3, CO_2CH_3), 3.60 (m, 4H, 8-CH_2), 3.65 (m, 4H, Acetal-OCH_2), 4.17 (t, 1H, Acetal-OCH_2), 4.26 (m, 2H, 17-H), 4.48 (m, 2H, 18-H), 4.60 (t, 1H, Acetal-OCH_2), 4.92, 5.08 (d, 4H, J=20 Hz, 13^2-H), 5.85 (m, 2H, Acetal-OCH_2), 6.84 (d, 2H, J=13 Hz, Acetal-OCH_2), 6.84 (s, 2H, 3-CH), 8.52 (s, 2H, *meso*-H), 9.29 (s, 2H, *meso*-H), 9.55 (s, 2H, *meso*-H). IR (KBr) ν_{max} 1733 (CO_2CH_3), 1690 cm^{-1} (C=O). MS (FAB) Found: m/z 1327. Calcd for $C_{71}H_{72}N_8O_{10}Zn_2$: M^+, 1327.

This work was partially supported by a Grant-in-Aid for Specially Promoted Research No. 02101005 from the Ministry of Education, Science and Culture. We thank Dr. I. Sakata of Toyo-Hakka Co., Ltd. for the kind gift of methyl pyropheophorbide *a*. We also thank Professor H. Tamiaki of Ritsumeikan University for his kind guidance in the preparation of pyropheophorbide and bacteriopyropheophorbide.

References

1) M. R. Wasielewski, *Chem. Rev.*, **92**, 435 (1992).
2) D. Gust, T. A. Moore, and A. L. Moore, *Acc. Chem. Res.*, **26**, 198 (1993).
3) K. Maruyama and A. Osuka, *Pure Appl. Chem.*, **62**, 1511 (1990); K. Maruyama, A. Osuka, and N. Mataga, *Pure Appl. Chem.*, **66**, 867 (1993).
4) M. R. Wasielewski, W. A. Svec, and B. T. Cope, *J. Am. Chem. Soc.*, **100**, 1961 (1978); M. R. Wasielewski, D. G. Johnson, and W. A. Svec, "Supramolecular Chemistry," ed by V. Balzani, Reidel, Amsterdam (1987), p. 255; D. G. Johnson, W. A. Svec, and M. R. Wasielewski, *Isr. J. Chem.*, **28**, 193 (1988); P. A. Liddell, D. Barrett, L. R. Makings, P. J. Pessiki, D. Gust, and T. A. Moore, *J. Am. Chem. Soc.*, **108**, 5350 (1986).
5) M. R. Wasielewski, "Energy and Electron Transfer in Covalently Linked Chlorophyll-Containing Donor–Acceptor Molecules," ed by H. Scheer, CRC Press, Florida (1991), Section 1.10, pp. 269—286.
6) A preliminary report: A. Osuka, S. Marumo, N. Konishi, K. Maruyama, I. Yamazaki, T. Yamazaki, Y. Shirakawa, and Y. Nishimura, *Chem. Lett.*, **1993**, 2141.
7) R. K. Harris, "Nuclear Magnetic Resonance Spectroscopy," Pitman, London (1983).
8) First we attempted to measure the 1D NOE difference spectra of **5** and **6**, but we could not detect any meaningful NOE effects. This can be ascribed to mismatching of the molecular weights of **5** and **6** (907) with a 500 Hz NMR machine.[7]
9) J. B. Birks, "Photophysics of Aromatic Molecules," Wiley-Interscience, London (1970).
10) H. Heitele, S. Finckh, S. Weeren, F. Pöllinger, and M. E. Michel-Beyerle, *J. Phys. Chem.*, **93**, 5173 (1989); G. L. Gaines, III, M. P. O'Neil, W. A. Svec, M. P. Niemczyk, and M. R. Wasielewski, *J. Am. Chem. Soc.*, **113**, 719 (1991).
11) T. Asahi, M. Ohkochi, R. Matsusaka, N. Mataga, R. P. Zhang, A. Osuka, and K. Maruyama, *J. Am. Chem. Soc.*, **115**, 5665 (1993).
12) Intramolecular electron-transfer events were observed by picosecond transient absorption spectroscopy, S. Taniuguchi, T. Okada, N. Mataga, A. Osuka, and Y. Wada, unpublished results.
13) A. Osuka, S. Nakajima, K. Maruyama, N. Mataga, T. Asahi, I. Yamazaki, Y. Nishimura, T. Ohno, and K. Nozaki, *J. Am. Chem. Soc.*, **115**, 4577 (1993).
14) M. R. Wasielewski and W. A. Svec, *J. Org. Chem.*, **45**, 1969 (1980).
15) T. Mukaiyama, M. Usui, and K. Saigo, *Chem. Lett.*, **1975**, 1163.